Journal of Insect Science (*2017*) 17(1); 20: 1–9
doi: 10.1093/jisesa/iew116
Research article

Morphology of the Male Reproductive System and Spermiogenesis of *Dendroctonus armandi* Tsai and Li (Coleoptera: Curculionidae: Scolytinae)

Yi-Fei Wu,[1] Lu-Sha Wei,[2] Mark Anthony Torres,[3] Xu Zhang,[1] Shao-Ping Wu,[1] and Hui Chen[1,4]

[1]College of Forestry, Northwest A&F University, Yangling, Shaanxi 712100, China (yifeiwu53@163.com; azhangxu1983@163.com; wushaoping@126.com; chenhui@nwsuaf.edu.cn), [2]College of Food engineering and nutritional science, Shaanxi Normal University, Xi'an, Shaanxi 710119, China (lusafei@163.com), [3]College of Science and Mathematics, Mindanao State University—Iligan Institute of Technology, Iligan City 9200, Philippines (torres.markanthony@gmail.com), and [4]Corresponding author, e-mail: chenhui@nwsuaf.edu.cn

Subject Editor: Stuart Wigby

Received 27 July 2016; Editorial decision 29 November 2016

Abstract

Studying the reproductive attributes of pests is central to understanding their life cycle history and in crafting management strategies to regulate, if not bring down, their population below threshold levels. In this article, the morphology of the male reproductive tract, topology of the spermatozoa, and salient features of spermiogenesis in the Chinese white pine beetle, *Dendroctonus armandi* Tsai and Li was studied to provide baseline information for further pest management studies. Results showed that male reproductive tract of this species differs from those documented in other Coleopterans by having 20 testicular tubules in each testis and the presence of two types of accessory glands. The spermatozoon is seen having peculiar characteristics such as an "h"-shaped acrosomal vesicle with a "puff"-like expansion, one centriole, one large spongy body, and two accessory bodies. Despite with some morphological differences of the male reproductive organ, spermatogenesis in this organism is similar to other Coleopterans. Overall, detailed studies regarding the components of the primary male reproductive organ of this beetle species would expand the knowledge on the less-understood biology of Coleopteran pests and would help in designing regulatory measures to conserve endemic and indigenous pine trees in China.

Key words: reproduction, Scolytidae, Dendroctonus armandi, spermatogenesis

In China, pine trees provide important forest cover in areas where deciduous trees cannot grow due to extreme elevation. There are a variety of pine trees in the country, but the most species rich is that of the genus *Pinus* (Mirov 1967, Price *et al.* 1998). While pine trees are widespread in parts of China, these trees are threatened by the presence of phytophagous insects, such as the bark beetles and other subcortical insects that feed as larvae and adults in the phloem of the tree (Wood and Bright 1992). The severity of the threat can be enormous considering that there are over five hundred species of phytophagous insects that feed on pine trees of the genus *Pinus* alone.

Aside from being an important forest cover, some species of pine trees are revered as cultural symbols. Such is the case of the Chinese White Pine, *Pinus armandi*, which is regarded by Chinese ethnology as an emblem of longevity and immortality. In fact, in several accounts in the history of the country, the resin of this species is consumed by Taoist seekers of immortality in the hope of prolonging their lives. Just like other conifers, this species is composed of morphologically distinct varieties that include the var. *armandi*, var. *mastersiana*, and var. *dabeshanensis*. Among the three, the var. *dabeshanensis* and var. *mastersiana* are considered by the International Union for the Conservation of Nature as vulnerable and endangered, respectively. While this species remains to be one of the culturally and ecologically important pine trees in China, its populations are threatened by infestation of the Coleopteran pest *Dendroctonus armandi*. According to Yin et al.(1984) and Chen and Yuan (2000), *D. armandi*, which is endemic in China, is tagged as the most destructive forest insect in the Qinling Mountains of northwest China. Historically, the native Chinese white pine has been severely damaged by the insect pest since 1953. This insect is known to selectively infest healthy *P. armandi* trees that are >30 years old (Chen and Yuan 2000, Chen and Tang 2007, Chen et al. 2010).

To protect *P. armandi* from succumbing to the insect pest, populations of *D. armandi* must be maintained at manageable levels

below the threshold. One way to do this is to control or regulate the reproductive behavior of the species in order to come up with species-specific intervention programs. This entails studying important aspects of the reproductive biology of the organism. So far, only a few aspects such as breeding preferences, frequency of oviposition, and the mating cycle of *D. armandi* have been studied (Yin et al. 1984, Chen and Yuan 2000). The reproductive tract, ultrastructural spermatogenesis, and spermatozoa of the species have not been described. According to Franzen (1955), studying sperm morphology is relevant to fertilization biology. Thus, the examination of sperm structure and morphological information is of significance in questions dealing with reproductive biology.

The sperm ultrastructure in the Coleopteran has been investigated in many different families (Jamieson 1987, Jamieson et al. 1999, Werner et al. 2002, Name et al. 2007, José et al. 2008, Paoli et al. 2014). Their sperms are found to basically match the classical pterygote type, which is characterized by the presence of a 9 + 9 + 2 axoneme, two accessory bodies and two mitochondrial derivatives (Tombes and Roppel 1972, Baccetti et al. 1973, Burrini et al. 1988, Báo 1996). Variations in the morphology of the spermatozoa can be attributed to species differentiation and in many cases can be used to distinguish among taxonomic groups (Burrini et al. 1988, Kôji 2007).

In light of the importance of studying the male reproductive biology of *D. armandi*, this study therefore was conducted to describe the gross morphology of the male reproductive tract, illustrate various stages of sperm formation, and determine the ultrastructural morphology of mature spermatozoon.

Materials and Methods

Insect Samples

Adult males of *D. armandi* were collected from the bark of infested *P. armandi* in the Huoditang Experimental Forest Station, Qinling Mountains (33° 18′–33° 28′ N, 108° 21′–108° 39′ E) in 13 July 2015, 30 insect samples were used in each developmental stage and the microstructure of the tissue samples were magnified via a stereomicroscope, the reproductive organs located near the dorsal vessel were removed and placed in Ringer's solution. This solution was used to preserve the integrity of the tissues.

Scanning Electron Microscopy

Tissue samples were fixed in 2.5% glutaraldehyde and buffered to pH 7.2 with 0.1 mole/liter phosphate solutions for 12 h at 4 °C. After washing the organs in phosphate buffer saline (PBS), pH 7.2, the samples were postfixed in 1% osmium tetroxide solution for 2 h at 4 °C, dehydrated through a graded series of acetone, critical-point-dried with liquid CO_2, and sputtered coated with gold (10-nm thick). Samples were then examined using the JEOL T330 SEM.

Transmission Electron Microscopy

Samples were fixed in 2.5% glutaraldehyde in 0.1 M sodium cacodylate buffer overnight at 4 °C, rinsed with PBS buffer at pH 7.2, postfixed in 1% osmium tetroxide for 2 h at 4 °C, and dehydrated in graded acetone series. The reproductive organs were then embedded in a mixture of Epon and Araldite. Ultrathin sections were generated using a diamond knife on a LKB ultramicrotome, contrasted with uranyl acetate and lead citrate and visualized using the JEOL 1200EX TEM.

Results

Gross Morphology of the Male Reproductive Tract

The male internal reproductive tract in *D. armandi* is composed of two units encapsulated by the scrotal membrane. Each unit is formed by a testis comprising 20 testicular tubules (seminiferous tubules), an efferent duct (which forms a seminal vesicle and inserted in the testis depression), and two accessory glands (curled gland and strand-shaped gland) (Fig. 1A and B). The curled gland is like a petal surrounding the vas deferens while the strand-shaped gland, located at the top of the curled gland, has a long branch and a short branch connected to the seminal vesicle. The units fuse at their ends flowing into an ejaculatory duct (Fig. 1A).

The testicular tubules of the sexually mature male insects are full of sperm cysts, within which spermatogenesis occurs (Fig. 1C and D). A cyst with big nuclei can be observed, which constitutes a group of germ cells surrounded by an epithelium. The number of spermatids per cyst is around 512 (Fig. 1D). Most mature sperms are stored in the seminal vesicle.

Spermatozoa Differentiation

Spermiogenesis in *D. armandi* involves processes such as nuclear elongation, chromatin condensation, and formation of structures such as the acrosome, axoneme, and the mitochondrial derivatives. The majority of cysts are filled with spermatids. Some secondary spermatocytes with ovoid nucleus and the gathering mitochondria are found in many testicular cysts of *D. armandi* (Figs. 1D, 2A and B).

The early spermatid nucleus is circular (3 μm in diameter) and contains heterogeneous chromatin with a granular appearance (Fig. 3A). During spermiogenesis, the spermatid nucleus changes shape, elongates, and develops a posterior lateral invagination (Fig. 3B). At the same period, the spherical-shaped mitochondria that are found dispersed in the cytoplasm begin to migrate toward the basal pole of the nucleus (Fig. 3A and B). The mitochondrion decreases in number but increases in size. Then, the complex aggregation of mitochondria occurs and forms one big Nebenkern (Fig. 3A–C). The Nebenkern splits into two equal mitochondria derivatives, which are surrounded by the microtubules (Fig. 3D).

At the mid-spermatids stage, the nucleus contains small dense aggregations of heterochromatin close to the peripheral region of the nuclear envelope. The nucleus gradually elongates, forming a trident-shaped structure (Fig. 4A and B). After which, there is a gradual condensation of nuclear chromatin as evidently observed by the increase of electron density in the region. Chromatin is more condensed around the periphery of the nucleus than at the center (Fig. 4A–F). Two distinguishable nuclear regions were observed: one has homogeneously condensed chromatin and the other has dispersed fibrillary chromatin (Fig. 4F). As spermiogenesis comes to an end, all spermatids are seen with scanty cytoplasm and completely condensed nucleus surrounded by a layer of microtubules (Figs. 5A–C and 6A). During the nucleus transformation, the two mitochondrial derivatives acquire different sizes and become laterally located in relation to the nucleus (Fig. 4C). The two mitochondrial derivatives are highly organized with well-developed cristae and dense crystalloid in the mitochondrial matrix (Figs. 4F and 5C).

Among early spermatids, the formation of the proacrosomal vesicle, which is derived from vesicles of the Golgi complex, can be observed. (Fig. 3A and C). In mid-spermatids, this vesicle, with an electron-dense granule, increases in size and develops into an acrosome, which covers the anterior pole of the spermatid nucleus (Fig.

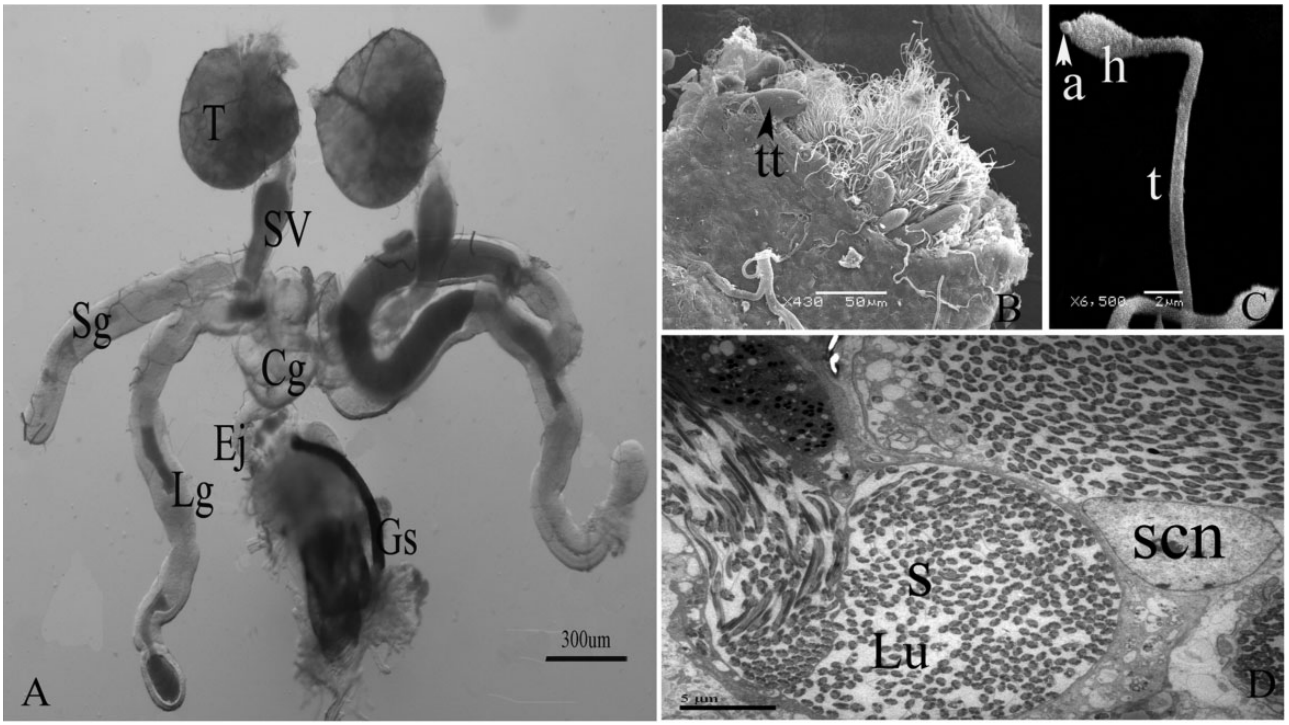

Fig. 1. The male reproductive organ and sperm cell of *D. armandi*. (**A**) Light micrograph showing the male reproductive organ, which is composed of testis, efferent duct, seminal vesicle, strand-shaped accessory gland, curly accessory gland and a common ejaculatory duct. (**B**) A scanning electron micrograph showing the testicular tubules of the testis. (**C**) A TEM of a mature sperm indicating the acrosome and nucleus of the head and a tail. (**D**) TEM image showing the cross section of the spermatocyst showing a prominently big nucleus and the approximately 512 spermatids in the lumen. a, acrosome; Cg, curly accessory gland; Ej, ejaculatory duct; Gs, gastric speculum; h, head of sperm; Lg, long branch of strand-shaped accessory glands; Lu, lumen of the cysts; s, spermatids; scn, nucleus of spermatocyst; Sg, short branch of strand-shaped accessory glands; SV, seminal vesicle; T, testis; t, tail of sperm; tt, testicular tubules.

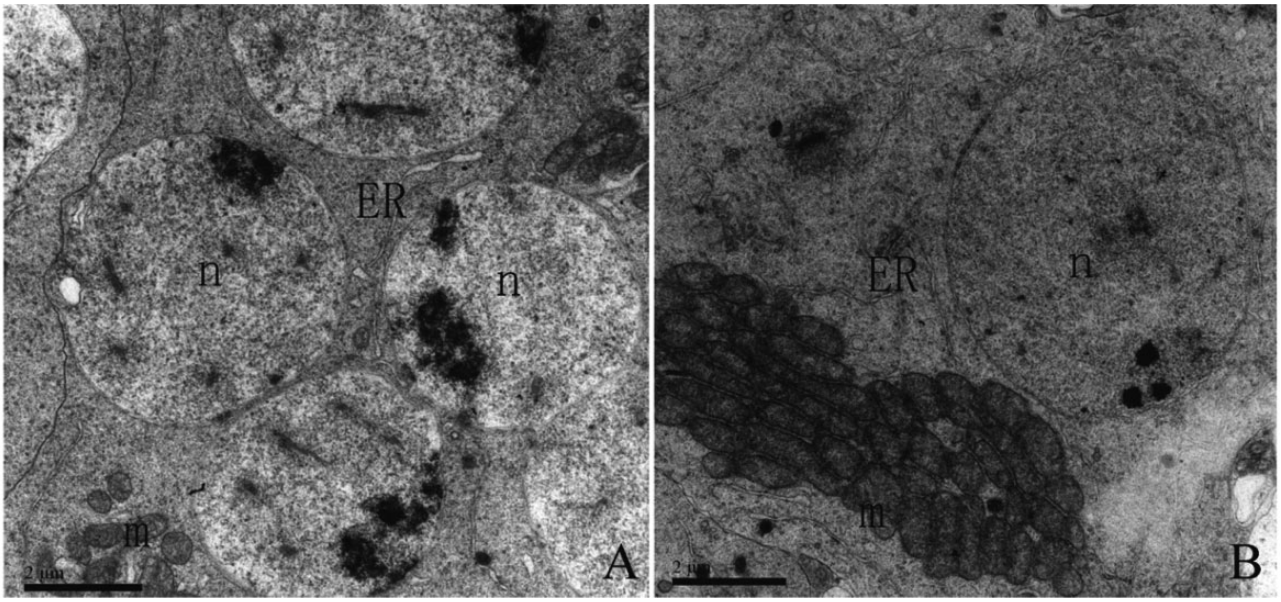

Fig. 2. Secondary spermatocytes in a testicular cyst of *D. armandi* (TEM images). (**A**) Several mitochondria are gathering proximal to the nuclei. (**B**) The elongated mitochondria have completely migrated lateral to the nuclei. ER, endoplasmic reticulum; m, mitochondria; n, nucleus.

4A and B). In more advanced spermatids, the acrosome differentiates to form a cone-shaped structure with an inner cavity (Fig. 4E). In transverse sections of the late-spermatids, the acrosomal vesicle is more or less triangular but becomes circular at the anterior tip (Figs. 5A and B). Formation of the "h"-shaped acrosomal vesicle is completed in the mature sperm (Fig. 6A).

During the early spermatid phase, the axonemal formation begins with a specific $9+9+2$ arrangement of the microtubules

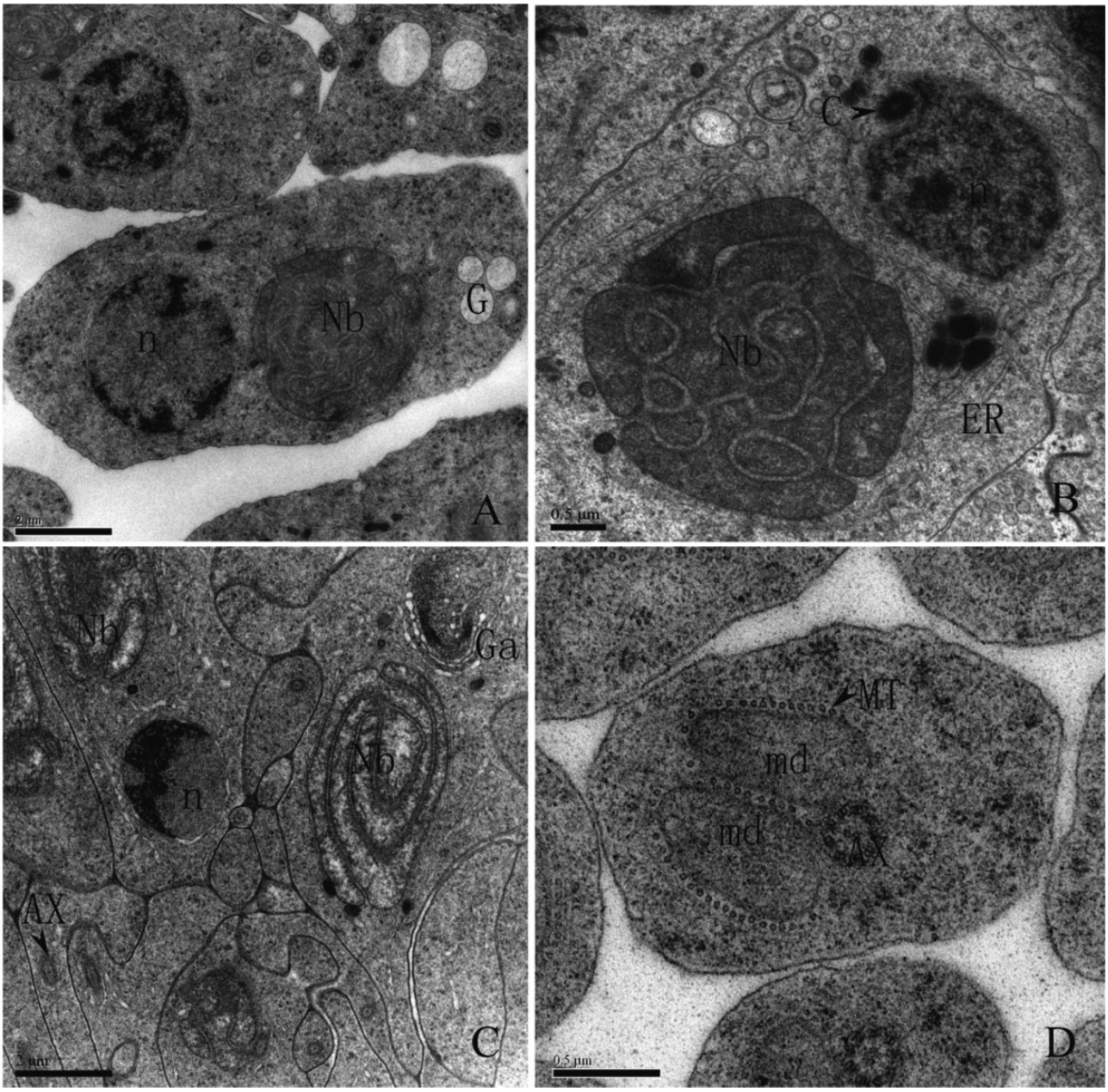

Fig. 3. Appearance of Nebenkern and formation of mitochondrial derivatives in early spermatid phase (TEM images). (**A**) An early spermatid characterized by dispersed chromatin in the nucleus and the presence of a Nebenkern. (**B**) The centriole in the concavity of the nucleus and a large Nebenkern. (**C**) Crescent-shaped Golgi apparatus. (**D**) Nebenkern divides into two mitochondrial derivatives along the axoneme. Many microtubules surround the mitochondrial derivatives and axoneme, and run parallel to the axoneme. AX, axoneme; C, centriole; ER, endoplasmic reticulum; G, Golgi body; Ga, Golgi apparatus; MD, mitochondrial derivatives; MT, microtubules; n, nucleus; Nb, Nebenkern.

(Fig. 3C and D). The axoneme, which is typical in sperms among beetles, originates from the centriole, emerges from the implantation fossa, and extends toward the distal pole of the cell (Fig. 4A and B). A mass of electron-dense material (centriolar adjunct) organizes a sheath around the centriole (Fig. 4D and E). The longitudinal section at the posterior region of the nucleus in the late-spermatids shows that the centriolar adjunct disappears and the axoneme terminates at the centriole in of the nuclear concavity (Fig. 5B and C). In longitudinal sections, the centriole appears to be moderately electron dense, uniformly compact, and approximately circular in shape (Fig. 6B).

Spermatozoa

Spermatozoa, which measured approximately 85 ± 11.3 μm ($n = 50$) in length, consist of two morphologically and functionally distinct regions: the head and the tail (or flagellum) (Fig. 1C). The sperm head is elliptical and formed by the nucleus and the acrosome. The nucleus, enveloped by the nuclear envelope, occupies most of the spermatozoon head and is mostly uniformly electron dense (Fig. 6A). The nuclear anterior part shows an oblique profile, in close association with the acrosomal complex region. In longitudinal sections, the nucleus is thicker (about 0.75 μm in diameter) at the

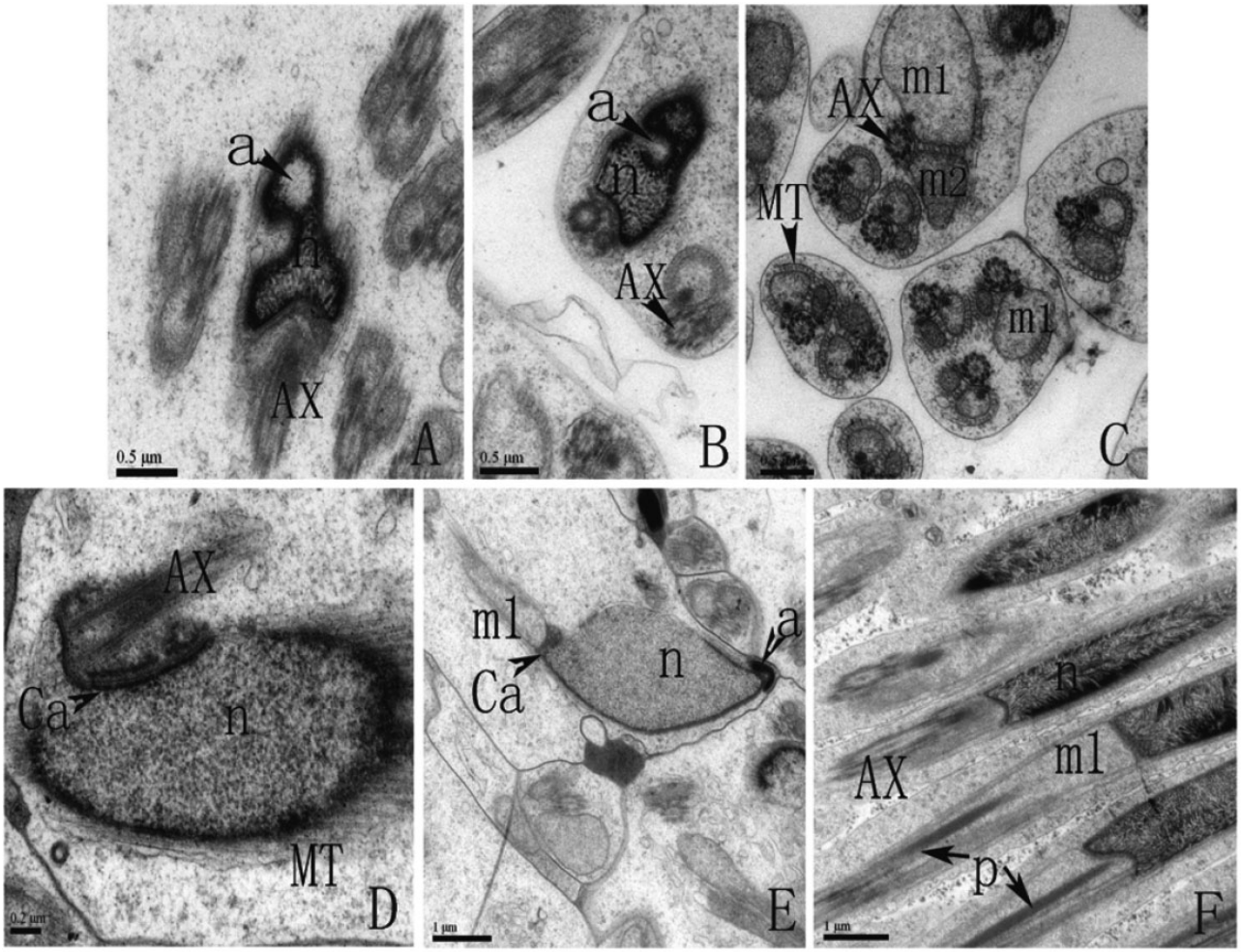

Fig. 4. Mid-spermatids of *D. armandi* (TEM images). (**A**) Transverse section of the sperm flagellum showing microtubules and an endomembrane surrounding the major and minor mitochondrial derivatives. (**B**) Longitudinal sections through the trident-shaped nucleus. The acrosome comes into close contact with the nucleus and is sometime located lateral to the nucleus. (**C**) The acrosome is located at the anterior part of the trident-shaped nucleus in longitudinal sections. (**D**) Electron-dense materials form a sheath (centriole adjunct) surrounding the centriole in longitudinal section. (**E**) The acrosome settles at its final position, and it differentiates to form a cone shape with an inner cavity. At the same time, electron-dense materials form a sheath (centriole adjunct) surrounding the centriole in longitudinal section. (**F**) The major mitochondrial derivative with a paracrystal has low electron-dense material, which overall causes a weak contrast in electron microscopic pictures. a, acrosome; AX, axoneme; Ca, centriole adjunct; m1, major mitochondrial derivative; m2, minor mitochondrial derivative; MT, microtubules; n, nucleus; p, paracrystal.

posterior end and tapers off toward the flattened anterior end (Fig. 6A and B).

The acrosomal complex is small, approximately 1 μm in length, and almost covers the anterior part of the nucleus (Fig. 6A). It is triple layered: a layer of extra-acrosomal material, an acrosomal vesicle with strong electron density, and internally the perforatorium. The asymmetrical acrosomal vesicle is cone shaped with a predominant strand tip and an appearance of "h"-shaped structure, which covers the axial rod up to the beginning of the nucleus.

The posterior end of the nucleus forms the concavity, which is the region of the centriole (Fig. 6B). At the junction of nucleus and flagellum, the conspicuous centriole is very compact and electron dense (Fig. 6B). This posterior region of centriole lies parallel to the anterior part of the axoneme and lies between the anterior tips of the mitochondrial derivatives (Fig. 6B).

The flagellum is characterized by the 9 + 9 + 2 microtubule pattern, which is typical among insects, two elongated mitochondrial derivatives, a pair of accessory bodies, a spongy body and a "puff"-like expansion (Fig. 6B–E). The axoneme originates from a differentiated centriole and presents the typical pattern of 9 (outer singlets) + 9 (intermediate doublets) + 2 (central singlets) microtubules (Fig. 6D). The two mitochondrial derivatives, which are laterally located in relation to the nucleus, are asymmetric in both length and diameter (Fig. 6C and D). There is a paracrystalline material in each mitochondrial derivative situated in the mitochondrial region adjacent to the axoneme (Fig. 6D). The major mitochondrial cristae are clearly visible in cross-sectional view. Regularly spaced mitochondrial cristae can be seen clearly in longitudinal sections, and the distance between the cristae is about 0.04 μm. The major mitochondrial derivatives begin with its tips lying near nuclear concavity and the minor mitochondrial derivatives with its tips lying between the axoneme and the posterior extremity of the centriole (Fig. 6B). Furthermore, one terminates just before the other and this one immediately above the axonemal tip (Fig. 6D).

Cross sections reveal that flanking the axoneme are two triangularly shaped accessory bodies (of unequal sizes). A "puff"-like expansion is seen parallel to the axoneme and closely adjacent to a smaller accessory body (Fig. 6D and E). Also, the spongy body, like

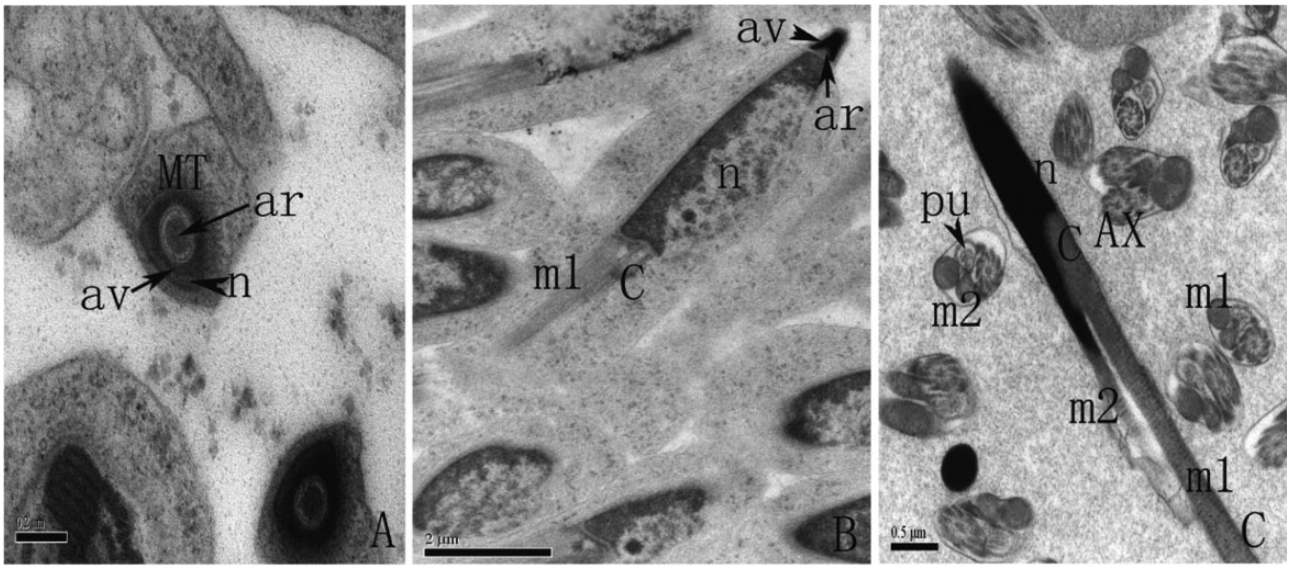

Fig. 5. The late-spermatids of *D. armandi* (TEM images). (**A**) Cross-sectional view of the acrosome showing an electron-dense outer sheath and an inner core and is surrounded by numerous microtubules. (**B**) Acrosome is transformed to an electron-dense outer sheath and an inner core in longitudinal sections. (**C**) The "puff"-like expansion is adjacent to a smaller accessory body and the rod-shaped centriole is located in the nuclear concavity in longitudinal sections. ab, accessory body; ar, axial rod; av, acrosomal vesicle; AX, axoneme; C, centriole; MT, microtubule; m1, the major mitochondrial derivative; m2, the minor mitochondrial derivative; n, nucleus; pu, puff"-like expansion.

a loose coil, can be seen as a large cluster of anastomosing canaliculi, and is located flanking to the anterior flagellum. At the end of the tail, the flagellar components terminate, starting with the accessory bodies, followed by the minor mitochondrial derivative, and lastly, the major mitochondrial derivative (Fig. 6D and E). The several microtubules of the axonemal complex are the last to disappear at different levels (Fig. 6D).

Discussion

Results of this study show that the general morphology of the male reproductive apparatuses of *D. armandi* is similar to the rest of the beetle species belonging to Suborder Polyphaga (Jamieson et al. 1999, Werner et al. 2002). This is characterized by a pair of testes, seminal vesicles, efferent ducts, accessory glands, and the ejaculatory ducts. However, nuances can be observed with regards to the number and morphology of the accessory glands, which considerably vary among Coleopterans. Distinctively, the accessory glands of *D. armandi* are morphologically characterized as paired curled glands and strand-shaped glands with long and short branches. This is in contrast to *Hypothenemus hampei* and *Tenebrio molitor*, where each has four accessory glands (Devasahayam et al. 1998, Tang et al. 2010), and to *D. monticolae*, which possess three pairs of accessory glands that are associated with spermatophore production (Cerezke 1964).

Similar to most insects, the development of the germinative cells in *D. armandi* takes place within cysts like most insects (Phillips 1970), and the mature spermatozoa are located at the seminal vesicle. The testes have three types of germ cells (secondary spermatocytes, spermatids, and nearly mature sperms) and appeared not deteriorated in the adult individual. These observations suggest that the production of sperms may continue until maturity. In each cyst, the number of spermatids varies among different species as a result of spermatogonial premeiotic divisions (Oguma et al. 1987, Quagio-Grassioto and Lello 1996). In Coleopterans, the number of sperm/bundle varies from 16 (2^4) to 512 (2^9), with 256 being the most common quantity (Jurečić 1988). For example, there are 16–256 spz/b (spermatozoa per bundle) among the alticid beetles, 256 spz/b in *Sitophilus zeamais* and *Sitophilus. Oryzae* (Name et al. 2007), and 512–797 spz/b in the bool weevil, *Anthonomus grandis* (Gassner *et al.* 1975). A hypothesis has been put forward that modern orders of insects have less sperms per bundle than the archaic orders (Virkki 1969, 1973). In this study, *D. armandi* has a high number of sperms per bundle (approximately 512 spz/b). This number would reflects that *D. armandi* is a primitive Coleopteran species. Spermiogenesis in *D. armandi* is characterized by specific morphofunctional modifications. However, elements universal among Coleopterans can be observed such as the changes in shape and chromatin condensation of the nucleus following the formation of the acrosome and flagellum (Shay et al. 1969, Gassner et al. 1975, Hodges 1982, Dybas and Dybas 1987, Báo et al. 1989, Báo 1996, Werner et al. 2002, Name et al. 2007). A peculiar nuclear shape and organization of the nuclear material can also be seen during the differentiation of spermatozoa in *D. armandi*. The chromatin condenses at the periphery, and the nucleus gradually elongates, forming a trident-shaped structure. After which, the nuclear chromatin gradually condenses from the periphery to the center. The nuclear chromatin then exhibits a more homogeneously condensed forms and a fibrillar aspect. Then, the more compact nucleus forms in the mature spermatids. These structural changes associated with nuclear development have been described in other beetles (Báo and Hamú 1993, Báo 1996) therefore not unique to *D. armandi*. Apparently, in *D. armandi*, a trident-shaped nucleus in mid-spermatids and a deep inner cavity in the posterior nuclear region, which hosts the centriole and the beginning of the axoneme, were clearly observed.

Ultrastructures of the spermatozoa have been reported in some Curculionoidea insects (Bedford and Millar 1978, Burrini et al. 1988, Werner et al. 1999, Báo and Hamú 1993, Werner et al. 2002, Name et al. 2007, Zizzari et al. 2008;). Spermatozoa in Kissophagus emoporus and Hederae fagi from subfamily Scolytidae are found to

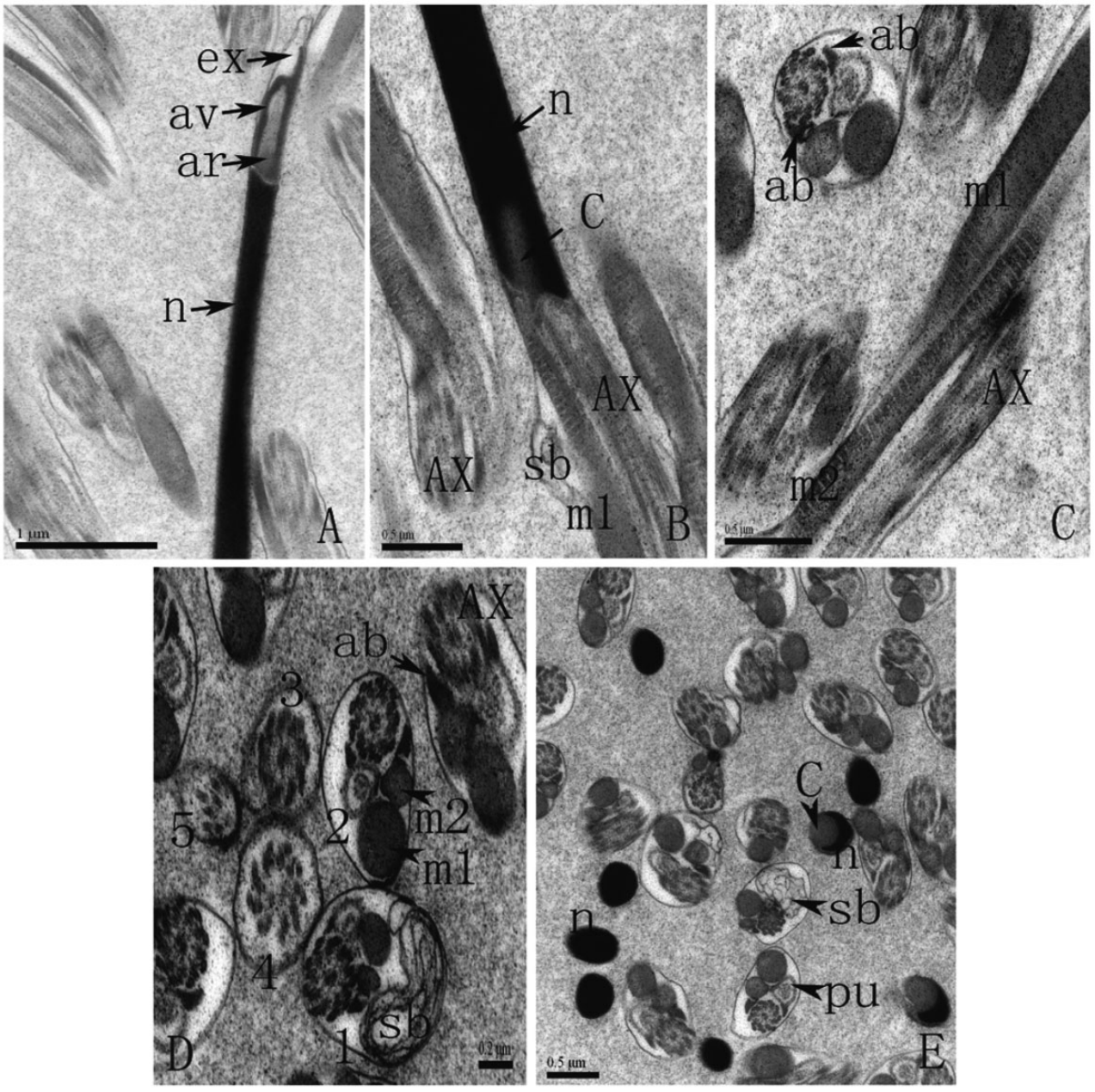

Fig. 6. TEM images of a mature sperm cell. (**A**) Longitudinal section of the sperm head showing the tri-layered acrosome consisting of an axial rod, a "h"-shaped acrosomal vesicle and an extra-acrosomal material (ex). (**B**) Longitudinal section of the posterior end of the nucleus. The spongy body appears as a loose "coil"-shaped structure flanking the anterior region of the flagellum. (**C**) Image of the longitudinal section of the tail. The axonome, major mitochondrial derivative and minor mitochondrial derivative exhibit a helical arrangement. (**D**) Transverse sections of the sperm flagellum. 1 shows the two accessory bodies, axoneme, spongy body, major mitochondrial derivative, minor mitochondrial derivative and the "puff"-like structure in the mid-piece of the sperm tail; 2 shows accessory bodies, axoneme, major mitochondrial derivative, minor mitochondrial derivative and the "puff"-like expansion in the principal piece of the sperm tail; 3 shows $9+9+2$ axoneme at the end piece of sperm tail; 4 shows the central singlet axoneme disappearing at the end of sperm tail; 5 shows loose nine outer microtubule fibers at the endmost piece of sperm tail. (**E**) Transverse sections of the sperm flagella. The spongy body is only present in the middle piece of sperm tail. The "puff"-like structure runs along the axoneme in the middle and principal piece of sperm flagella. ab, accessory body; ar, axial rod; av, acrosomal vesicle; AX, axoneme; C, centriole; ex, extra-acrosomal material; m1, the major mitochondrial derivative; m2, minor mitochondrial derivative; n, nucleus. sb, spongy body; pu, puff"-like expansion.

be similar to other Curculionoidea insects with a few variations (Burrini *et al.* 1988). The basic structural features seen in the spermatozoa of *D. armandi* are similar to most curculionids. A mature spermatozoon in *D. armandi* consists of 1) a three-layered acrosome, 2) two accessory bodies of different sizes, 3) a "puff"-like expansion, 4) two elongate mitochondrial derivatives of unequal length, with clearly distinguishable cristae, and 5) an axoneme with the typical $9+9+2$ arrangement of microtubules. Like in most Scolytinae spermatozoa (Burrini et al. 1988), the extra-acrosomal material in the acrosomes of *D. armandi* is poorly visible and almost absent in some cases. Interestingly, the primary differences of *D. armandi* spermatozoa compared to other curculionids are on the

topology of the acrosome, the presence of a single centriole, and the spongy body in the anterior tail.

In *D. armandi*, the acrosome has three layers: an extra-acrosomal amorphous layer, an acrosomal vesicle, and an axial rod or perforatorium. This structure of acrosome is typical in many coleopterans, such as the rove beetle (Werner et al. 2002), the rice weevil (Name et al. 2007), and the feather wing beetle (Dybas and Dybas 1987). However, the "h"-shaped acrosomal vesicle in *D. armandi* is distinct from those of other Coleopteran species, which have a cone-shaped acrosomal vesicle (Báo 1996, Name et al. 2007, Zizzari et al. 2008, Moreira et al. 2010). The thinner acrosomal vesicle has a more prominent tip that is about one fourth the length of the acrosomal vesicle, in contrast to *Kissophagus emoporus* and *Hederae fagi* (Burrini et al. 1988). Thus, the shape of thus acrosomal vesicle may be an important characteristic to be considered in phylogenetic studies.

A peculiar characteristic of the *D. armandi* spermatozoon is the presence of a single derived centriole. This unitary centriole exists among mature sperms, while the centriolar adjunct is only present in the early spermatid stage. Similarly, the centriolar adjunct is absent in the mature sperms of *Tenebrio molitor* (Baccetti *et al.* 1973), *A. grandis* (Gassner et al. 1975), and *Sitophilus zeamais* and *S. oryzae* (Name *et al.* 2007). The centriolar adjunct is organized by the accumulation of strong electron-dense material around the centriole in other coleopteran sperms (Breland et al. 1966; Phillips 1970; Mackie and Walker 1974; Werner 1976; Werner et al. 1999, 2002; Kubo-Irie et al. 2000;). In *D. armandi*, the centriole is considered to serve as a mechanical connection that stabilizes the insertion of the axoneme at the nuclear base. Two accessory bodies with a "puff"-like expansion may function as a stabilizer and as an organelle that assists the movement in coordination with the centriole.

Another unique feature of the *D. armandi* spermatozoon is the presence of a pronounced spongy body. This structure exists among late spermatids and mature sperms. It is located in the anterior tail and forms a superficial protrusions due to an extension of the spongy body. A similar structure has been reported in the spermatids of *Carpoglyphus lactis* (Acari: Astigmata) (Florek and Witaliński 2010). In *C. lactis*, the large cluster of spongy body is formed by an excess of spongy layer membranes. Contrasting to *C. lactis*, the origin of the spongy body in *D. armandi* has no spongy layer membranes. Dallai et al. (2005) reported that there were two membranous sacs in a similar place adhering to the mitochondrial derivatives in *Galloisiana yuasai* (Insecta, Grylloblattodea). The authors did not refer to the origin of membranous sacs, which are different from the shape of the spongy body in *D. armandi*. Likewise, in a similar place, the annulus of the midpiece gets wider and swollen in the manatee spermatozoa (Miller et al. 2001). Miller et al. (2001) suggested that the annulus could be the location of tail separation. Compared with that of *D. armandi*, the spongy body function is presumed to be for splitting the tail from the head during the process of sperm-oocyte interaction and fertilization, but the functional significance of such prominent structure remains unclear. This feature would be worthy of attention in future analyses, especially for phylogenetic purposes.

In conclusion, the spermatozoa and spermiogenesis of *D. armandi* reveal both general and group-specific characteristics shared among Coleopterans. Importantly, unique structures to *D. armandi* spermatozoa include the long "h"-shaped acrosomal vesicle, one centriole, one "puff"-like expansion, and a spongy body. Furthermore, the presence of 20 testis tubules and two types of accessory glands in *D. armandi* differ from other Coleopteran species so far examined. Although the precise functions of these unique structures are yet unknown, this discovery not only expands the taxonomic and phylogenetic studies of the subfamily Scolytinae but also provides insights into their physiological attributes in insemination and copulation specificity and selectivity.

Acknowledgments

We acknowledge the financial support of the National Natural Science Foundation of China (31670658) and the Program for Changjiang Scholars and Innovative Research Team in University of China (IRT1035). All the authors are especially grateful to the Qinling National Forest Ecosystem Research Station, Northwest A&F University, for providing laboratory facilities.

References Cited

Baccetti, B., A. G. Burrini, R. Dallai, F. Giusti, M. Mazzini, T. Renieri, F. Rosati, G. Selmi. 1973. Structure and function in the spermatozoon of *Tenebrio molitor*. The spermatozoon of Arthropoda XX. J. Mechanochem. Cell Motil. 2: 149–161.

Báo, S. N. 1996. Spermiogenesis in *Coelomera lanio* (Chrysomelidae: Galerucinae) ultrastructural and cytochemical studies, pp. 119–32. *In* P. Jolivet, M. L. Cox (eds.), Chrysomelidae biology: general studies. Academic Publishers, Netherlands.

Báo, S. N., and C. Hamú. 1993. Nuclear changes during spermiogenesis in two chrysomelid beetles. Tissue Cell. 25: 439–445.

Báo, S. N., I. Quagio-Grassioto, and H. Dolder. 1989. Acrosome formation in *Ceratitis capitata* (Diptera: Tephritidae). Cytobios. 58: 93–100. PMID:2805814

Bedford, J. M., and R. P. Millar. 1978. The character of sperm maturation in the epididymis of the *Ascrotal hyrax*, *Procavia capensis* and *armadillo*, *Dasypus novemcinctus*. Biol. Reproduction. 19: 396–406.

Breland, O. P., G. Gassner, R. W. Riess, and J. J. Biesele. 1966. Certain aspects of the centriole adjunct, spermiogenesis, and the mature sperm of insects. Can. J. Genet. Cytol. 8: 759–773.

Burrini, A. G., L. Magnano, A. R. Magnano, C. Scala, and B. Baccetti. 1988. Spermatozoa and phylogeny of Curculionoidea (Coleoptera). Int. J. Insect Morphol. Embryol. 17: 1–50. doi: 10.1016/0020-7322(88)90029-3

Cerezke, H. F. 1964. The morphology and functions of the reproductive systems of *Dendroctonus monticolae* Hopk. (Coleoptera: Scolytidae). Can. Entomologist. 96: 477–500.

Chen, H., and F. Yuan. 2000. Chinese white pine bark beetle ecosystem and integrated pest management in Qinling Mountain, pp. 2–10. China Forestry Publishing House, Beijing. (in Chinese).

Chen, H., Z. Li, and M. Tang. 2010. Laboratory evaluation of flight activity of *Dendroctonus armandi* (Coleoptera: Curculionidae: Scolytinae). Can. Entomologist. 142: 378e387.

Chen, H., and M. Tang. 2007. Spatial and temporal dynamics of bark beetles in Chinese white pine in Qinling Mountains of Shaanxi Province, China. Environ. Entomol. 36: 1124–1130.

Dallai, R., R. Machida, T. Uchifune, P. Lupetti, and F. Frati. 2005. The sperm structure of *Galloisiana yuasai* (Insecta, Grylloblattodea) and implications for the phylogenetic position of Grylloblattodea. Zoomorphology. 124: 205–212.

Devasahayam, S., P. S. P. V. Vidyasagar, and K. M. A. Koya. 1998. Reproductive system of pollu beetle, *Longitarsus nigripennis* Motschulsky (Coleoptera: Chrysomelidae), a major pest of black pepper, *Piper nigrum* Linnaeus. J. Entomol. Res. 22: 77–82.

Dybas, L. K., and H. Dybas. 1987. Ultrastructure of mature spermatozoa of a minute featherwing beetle from Sri Lanka (Coleoptera, Ptiliidae: Bambara). J. Morphol. 191: 63–76.

Florek, M., and W. Witaliński. 2010. Spermatogenesis and sperm structure in *Carpoglyphus lactis* (L.) (Acari: Astigmata). Arthropod Struct Dev. 39: 41–51.

Franzen, A. 1955. Comparative morphological investigation into the spermatogenesis among Mollusca. Zoologiska Bidrag Fran Uppsala. 30: 339–456.

Gassner, G., D. Childrem, and D. J. Klemetson. 1975. Spermiogenesis in boll weevil *Anthonomus grandis* Boheman (Coleoptera:Curculionidae). Int. J. Insect Morphol. Embryol. 4: 15–25.

Hodges, R. J. 1982. Ultrastructure of the somatic and germ cells of the testes of *Dermestes frischii* Kugelann (Coleoptera: Dermestidae). Int. J. Insect Morphol. Embryol. 11: 235–253.

Jamieson, B. G. M. 1987. The ultrastructure and phylogeny of insect spermatozoa. Cambridge University Press, Cambridge, Great Britain.

Jamieson, B. G. M., R. Dallai, and B. A. Afzelius. 1999. Insects: their spermatozoa and phylogeny. Science Publishers, New Hampshire.

José, D., G. Rubio, E. Alex, P. Bustillo, F. Luis, and E. Vallejo. 2008. Alimentary canal and reproductive tract of *Hypothenemus hampei* (Ferrari) (Coleoptera: Curculionidae, Scolytinae). Neotrop. Entomol. 37: 143–151.

Jurečić, R. 1988. Sperm cell number per bundle in *Gnorimus nobilis* L. (Coleoptera, Scarabaeidae). Genetica. 76: 27–31.

Kôji, S. 2007. Sperm bundle and reproductive organs of carabid beetles tribe Pterostichini (Coleoptera: Carabidae). Naturwissenschaften. 94: 384–391.

Kubo-Irie, M., I. Miura, M. Irie, T. Nakazawa, and H. Mohri. 2000. Spermiogenesis in the stag beetle, *Aegus lavicollis* Waterhouse (Coleoptera: Lucanidae), with special reference to the centriole adjunct. Invertebr. Reprod. Dev. 37: 223–231.

Mackie, J. B., and M. H. Walker. 1974. A study of the conjugate sperm of dytiscid water beetles *Dytiscus marginalis* and *Colymbetes fuscus*. Cell Tissue Res. 148: 505–519.

Miller, D. L., M. M. Dougherty, and S. J. Decker. 2001. Ultrastructure of the Spermatozoa from a Florida Manatee (*Trichechus manatus latirostris*). Anat Histol Embryol. 30: 253–256.

Mirov, N. T. 1967. The genus Pinus. The Ronald Press Company, New York.

Moreira, J., V. A. Araujo, S. N. Bao, and J. Lino-Neto. 2010. Structural and ultrastructural characteristics of male reproductive tract and spermatozoa in two Cryptinae species (Hymenoptera: Ichneumonidae). Micron. 41: 187–192.

Name, K. P. O., G. P. F. Dos Reisand, and S. N. Bao. 2007. An ultrastructural study of spermiogenesis in two species of *Sitophilus* (Coleoptera: Curculionidae). Biocell. 31: 229–236.

Oguma, Y., H. Kurokawa, and T. Kusama. 1987. Number of primary spermatocytes in the *Drosophila immigrans* (Sturtevant) group (Diptera: Drosophilidae). Int. J. Insect Morphol. Embryol. 16: 85–89.

Paoli, F., R. Dallai, M. Cristofaro, S. Arnone, V. Francardi, and P. F. Roversi. 2014. Morphology of the male reproductive system, sperm ultrastructure and gamma-irradiation of the red palm weevil *Rhynchophorus ferrugineus* Oliv. (Coleoptera: Dryophthoridae). Tissue Cell. 46: 274–285.

Phillips, D. M. 1970. Insect sperm: their structure and morphogenesis. J. Cell Biol. 44: 243–277. PMCID: PMC2107952

Price, R. A., A. Liston, and S. H. Strauss. 1998. Phylogeny and systematics of *Pinus*. *In* D. M. Richardson (eds.), Ecology and biogeography of pinus. Cambridge University Press, Cambridge.

Quagio-Grassioto, I., and E. Lello. 1996. Cytoplasmic bridges, intercellular junctions, and individualization of germ cells during spermatogenesis in *Dermatobia hominis* (Diptera, Cuterebridae). J. Morphol. 227: 145–154.

Shay, J. W., E. E. Simmons, and W. J. Dobson. 1969. Notes on the male germ cells of a beetle, *Leptinotarsa decemlineata*. Entomol. News. 80: 185–191.

Tang, J., Y. Liu, M. Liu, and K. Cai. 2010. Study on the male reproductive system of *Tenebrio molitor*. J. Anhui Agri. Sci. 38: 2886–2887. (in Chinese).

Tombes, A. S., and R. M. Roppel. 1972. Ultrastructure of the spermatheca of the granary weevil, *Sitophilus granarius* (L.) (Coleoptera: Curculionidae). Int. J. Insect Morphol. Embryol. 1: 141–152.

Virkki, N. 1969. Sperm bundle and phylogenesis. Z Zellfisiol. 101: 13–27.

Virkki, N. 1973. Evolution of sperm cell number per bundle in insects. An. Esc. Nac. Cienc. Biol. Mexico 20: 23–34.

Werner, G. 1976. Entwicklung und Bau der Doppelspermien bei den *Dytisciden Acilius sulcatus* L., *Dytiscusmarginalis* L., und *Hydaticus transversalis* Pont. (Coleoptera). Zoomorphologie. 83: 49–87.

Werner, M., D. Zissler, and K. Peschke. 1999. Structure and energy pathways of spermatozoa of the rove beetle *Aleochara bilineata* (Coleoptera: Staphylinidae). Tissue Cell. 31: 413–420.

Werner, M., T. Tscheulin, T. Speck, D. Zissler, and K. Peschke. 2002. Ultrastructure and motility pattern of the spermatozoa of *Aleochara curtula* (Coleoptera, Staphylinidae). Arthropod. Struct. Dev. 31: 243–254.

Wood, S. L., and D. E. Bright. 1992. A Catalog of Scolytidae and Platypodidae (Coleoptera), Part 2, Taxonomic index, vol A. *Great Basin Naturalist*, (No. 13), 833 pp.

Yin, H. F., F. S. Huang, and Z. L. Li. 1984. Economic Insect Fauna of China, Vol. 29: Coleoptera: Scolytidae, Science Press: Beijing, China (in Chinese).

Zizzari, Z. V., P. Lupetti, C. Mencarelli, and R. Dallai. 2008. Sperm ultrastructure and spermiogenesis of Coniopterygidae (Neuroptera, Insecta). Arthropod Struct. Dev. 37: 410–417.